J. Phys. B: At. Mol. Opt. Phys. 26 (1993) 957–963. Printed in the UK

Fluorescence yields of high-lying doubly excited states of Ar^{16+}

Z Chen and C D Lin

Department of Physics, Kansas State University, Manhattan, KS 66506-2601, USA

Received 17 August 1992, in final form 11 January 1991

Abstract. The radiative and Auger decay rates of high-lying doubly excited states of multiply charged ions are calculated using wavefunctions obtained from the configuration interaction method. The fluorescence yields of all the states within the intrashell and intershell manifolds are examined and ordered in terms of the correlation quantum numbers. It is shown that the fluorescence yields of certain classes of intershell doubly excited states are quite large which are used to interpret the recent experimental observation of large average fluorescence yield of doubly excited states formed in collisions of multiply charged ions with atoms.

1. Introduction

Collisions of highly charged ions with atoms, molecules or surfaces are known to populate doubly or multiply excited states by double or multiple electron capture processes (Barat and Roncin 1992). These excited states stabilize by electron or photon emission. Consider the double capture process; if the charge state of the incident ion q is small (say $\leqslant 6$), then the doubly excited states formed decay primarily by the Auger process. In recent years, with multiply charged ions from EBIS sources, double electron capture processes have been shown to result in doubly excited states where the principal quantum numbers of the two electrons are quite large. Experimental results indicate that the average fluorescence yield of these states is quite large. For example, recent data by Cederquist *et al* (1992) showed that the average fluorescence yield can reach 0.2–0.4 for xenon ion projectile for q =30–40. Similar results have been obtained for other collisions (Ali *et al* 1992).

Low-lying doubly excited states of atoms and ions are best designated by ${}_n(K,T)^A_N$ quantum numbers, in addition to the usual quantum numbers L, S and parity π (Lin 1986). Here K, T and A are a set of integers that describe the correlation of doubly excited states and n and N are the approximate principal quantum numbers of the outer and inner electrons, respectively. For high-lying doubly excited states where $n, N \gg 1$, states from different (N,n) manifolds can become nearly degenerate and the intershell mixing between these states should be included. Consider, for example, the doubly excited states of Ar^{16+}. The states in the $(5,5)$ manifold overlap with the doubly excited states of the $(4,8)$ and $(4,9)$ manifolds. Thus the true eigenstates cannot be described by a single (N,n).

In a high-resolution spectrum, the result of the mixing between resonances from different manifolds is that the broad intrashell resonance exhibits modulations due to its interference with the narrower intershell resonances. Such modulations from overlapping resonances have been observed in the high-resolution photoabsorption

0953-4075/93/050957+07$07.50

spectra in helium recently (Domke *et al* 1991) and sophisticated theoretical methods have been developed to interpret such effects (Tang *et al* 1992). For ion–atom collisions, the energy resolution is not enough to resolve individual states. In fact, in most experiments, only the relative total radiative versus Auger branching ratio has been determined through the measurement of the charge state of the projectile ions after the collision. Thus, in the present study, our goal is not to consider the effect of overlapping resonances. Rather, our intention is to find a plausible interpretation of the large *average* fluorescence yield of doubly excited states formed from high-q incident ions. In this article, we study the fluorescence yields of high-lying doubly excited states for $n, N \geqslant 5$. We will neglect the coupling between states from different manifolds (different N) and calculate the fluorescence yield of states within a given manifold where each state is designated by the quantum numbers ${}_n(K,T)^A_N$ for each L, S and π. Thus the correlation within a manifold is included but the mixing due to different manifolds is not. We expect that the results from such calculations not be very accurate for each individual state, but the average fluorescence yield for each manifold will be very acceptable. In fact, this intershell mixing will affect the Auger rates of the $A = +$ states by up to a factor of two. Since the radiative rates for these states are small, the mixing does not increase or decrease the fluoresence yield significantly. The radiative rates are not very sensitive to the intershell mixing in general. Our goal is not to obtain an accurate fluoresence yield on each individual state, but to identify doubly excited states which have large fluorescence yields and that these states are formed in ion–atom collisions.

The radiative and Auger decay rates of high-lying doubly excited states follow certain propensity rules. These rules have been examined for a number of intrashell doubly excited states for the Ar^{16+} (6,6) manifold by Gou *et al* (1991). In this work, we will focus on the total radiative and Auger decay rates of a large number of intrashell and intershell doubly excited states. Section 2 describes briefly the computational methods. The results are presented and discussed in section 3 where both intrashell states and intershell states are considered and analysed in terms of the K, T and A quantum numbers. A brief summary is given in section 4.

2. Computational methods

The calculation of radiative and Auger rates is carried out using the standard configuration interaction (CI) method. This method is expected to be accurate for doubly excited states of positive ions and has the advantage that the method is stable and that a large number of states can be obtained at the same time. We note that calculations based on the average configuration method do not give reliable results for the radiative and Auger rates (Luc-Koenig and Bauche 1990). In the CI method, each wavefunction is expressed as the linear combination of the (anti)symmetrized product of hydrogenic wavefunctions

$$\Psi(r_1, r_2) = \sum_{n_1 l_1 n_2 l_2} C^{LMS}_{n_1 l_1 n_2 l_2} \Phi^{LMS}_{n_1 l_1 n_2 l_2}(r_1, r_2) \tag{1}$$

where

$$\Phi^{LMS}_{n_1 l_1 n_2 l_2}(r_1, r_2) = \frac{1}{\sqrt{2}} \left(R_{n_1 l_1}(r_1) R_{n_2 l_2}(r_2) Y^{LM}_{l_1 l_2}(\hat{r}_1, \hat{r}_2) \right.$$
$$\left. + (-1)^S R_{n_1 l_1}(r_2) R_{n_2 l_2}(r_1) Y^{LM}_{l_1 l_2}(\hat{r}_2, \hat{r}_1) \right) . \tag{2}$$

In (2), $R_{n_1 l_1}(r)$ is the radial hydrogenic wavefunction and $Y^{LM}_{l_1 l_2}(\hat{r}_1, \hat{r}_2)$ is the coupled spherical harmonics of the two electrons. The coefficients $C^{LMS}_{n_1 l_1 n_2 l_2}$ and the energies are determined by diagonalizing the Hamiltonian matrix using these basis functions. For the initial doubly excited state wavefunctions where the principal quantum numbers are about the same, the nuclear charge Z is used for the orbitals of both electrons. In calculating the radiative rates, where the principal quantum numbers of the final state wavefunctions of the two electrons are quite different, the inner electron sees a charge Z and the outer electron sees a charge $Z - 1$. The non-orthogonality of the hydrogenic orbitals is accounted for in the calculation of transition rates.

The radiative rates are calculated using the dipole approximation. The rates are averaged over the initial magnetic substates M_i and summed over all the final magnetic substates M_f,

$$W_R(10^{12}\ \mathrm{s}^{-1}) = 41.2 \times 10^3 \alpha^3 \omega_{if}^2 \frac{1}{2L_i + 1} \sum_{M_i, M_f} \tfrac{2}{3}\omega_{if} |\langle \Psi_f | r_1 + r_2 | \Psi_i \rangle|^2 \tag{3}$$

where ω_{if} is the energy separation, and Ψ_i and Ψ_f are the initial and final state wavefunctions, respectively.

The Auger rates are calculated by the standard formula,

$$W_A(10^{12}\ \mathrm{s}^{-1}) = 20.6 \times 10^3 4\pi |\langle \Psi_f^c | r_{12}^{-1} | \Psi_i \rangle|^2 \tag{4}$$

where the final state wavefunction Ψ_f^c is taken as the product of a bound and a continuum single electron wavefunction.

For each initial doubly excited state, there are many possible final radiative and Auger final states. The total radiative and Auger rates are obtained by summing over all partial radiative and Auger rates, respectively.

Equation (3) shows that radiative decays favour transitions with large photon energies, thus the dominant radiative channels result in states in the $(1, n)$, $(2, n)$ and $(3, n)$ manifolds initially. If these initial transitions end up in the $(2, n)$ and $(3, n)$ manifolds, these states will decay primarily by radiative transitions to even lower states, with little contribution to Auger processes. For the Auger decays, the transition is primarily to the channels where the continuum electron energy is small. The quasi-selection rule for the radiative and Auger decays has been examined in Gou *et al* (1991).

3. Results and discussions

First, we show in figure 1 the energy diagram of the $(4, n)$, $(5, n)$ and $(6, n)$ doubly excited states of Ar^{16+}. Since the number of states within each manifold is quite large, only the lowest and the highest levels are shown as horizontal bars, with all the other states lying in between. When the energy spread is small, a single bar is used to represent a manifold. The broken lines represent the ionization thresholds of Ar^{17+}. Notice that the $(5,5)$ manifold overlaps with the $(4,8)$ and $(4,9)$ manifolds, and the $(5,6)$ manifold overlaps with the Rydberg levels that converge to the $N = 4$ threshold. Similar overlap is evident for the $(6,6)$ and $(6,7)$ manifolds with the $(5, n)$

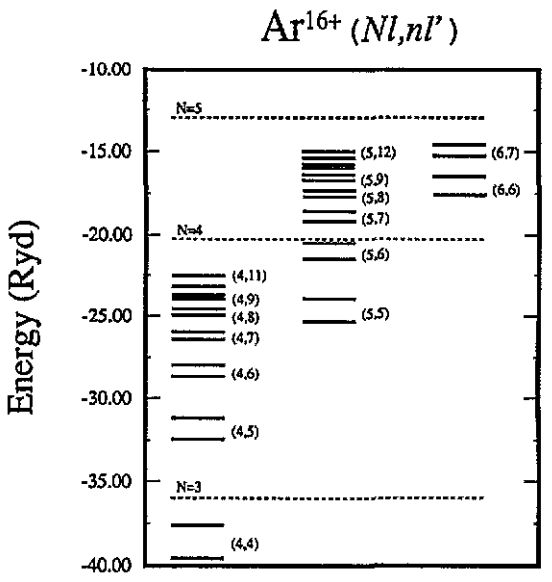

Figure 1. Energy level diagram of $Ar^{16+}(Nl, nl')$. Only the lowest and highest energy levels of the doubly excited states within each manifold are shown by full bars. When the energy spread within each manifold becomes small, a single full bar is used to represent that manifold. The broken lines are the one-electron ionization thresholds.

manifolds. These degeneracies imply that intershell mixing from different manifolds is large.

We first consider the fluorescence yield ω of intrashell states. In figure 2 we show the calculated results for the $(4,4)$ manifold. The fluorescence yield shows some regularity which has to do with the correlation pattern of doubly excited states. Such regularity has been studied for individual states by Gou *et al* (1991). We note that ω for each of the $K > 0$ states is small if $\eta = \pi(-1)^L = +1$. For $K < 0$ states, the fluorescence yields ω are large. If $\eta = -1$, then ω is large. We have checked that the radiative rates for all the states are nearly equal, but the Auger rates differ significantly owing to the significant role of electron correlation in the Auger decay. Auger rates cannot be calculated without proper account of electron correlations.

The fluorescence yield ω for intrashell states decreases rapidly with increasing N. In figures 3 and 4 we show the results for the $(5,5)$ and $(6,6)$ manifolds. From these results, one can extrapolate that the fluorescence yields of high-lying intrashell states are small in general. The relative values of ω still depend on the quantum numbers K and η.

We next consider the fluorescence yields of intershell states. For intershell doubly excited states, the quantum number A can have values of $+1$, -1 and 0 (all intrashell states have $A = +1$). From earlier works on doubly excited states, it is generally known that the Auger rates for $A = -1$ states are much smaller than the $A = +1$ states, while $A = 0$ states are much smaller than the $A = -1$ states. In figure 5 the fluorescence yields for states with $A = +1$ are shown with full symbols, while for $A = -1$ and $A = 0$ states are shown with open symbols. It is obvious that most of the $A = -1$ and 0 states have much larger ω in comparison with $A = +1$ states. The reason again is that the radiative rates are roughly comparable, but the Auger

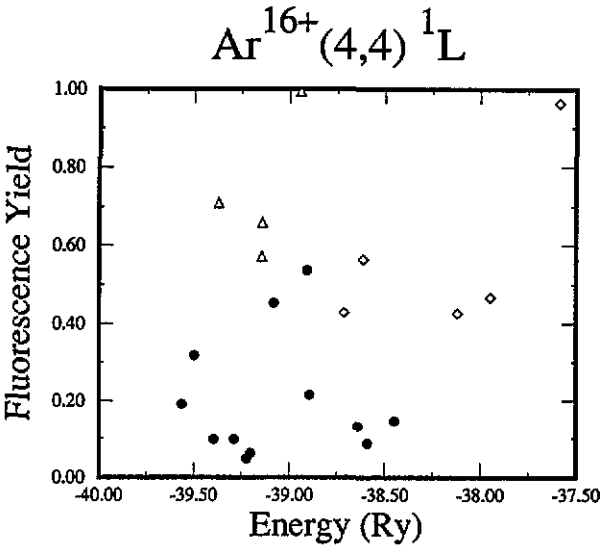

Figure 2. The fluorescence yields of all the singlet states of $(4,4)$ manifold of Ar^{16+}. They are plotted according to the total binding energy of the states. The full circles are for states with $K > 0$ and $\eta = +$, the open triangles are for states with $K > 0$ and $\eta = -$, and the open diamonds are for states with $K < 0$ and $\eta = +$.

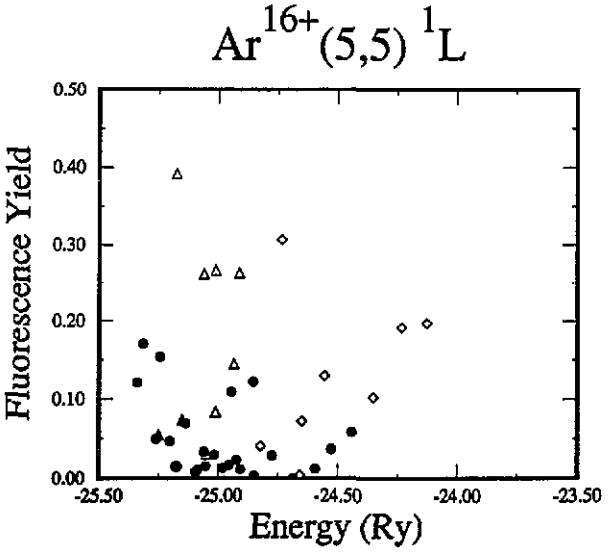

Figure 3. The same as figure 2, but for the $(5,5)$ manifold of Ar^{16+}.

rates are orders of magnitude different for $A = +1, -1$, and 0 states. This result is shown for the $(5,6)$ manifold in figure 5, but it is expected to be true for any intershell state.

The large number of $A = -1$ and $A = 0$ intershell states with large fluorescence yields may provide an explanation for the large average fluorescence yields observed

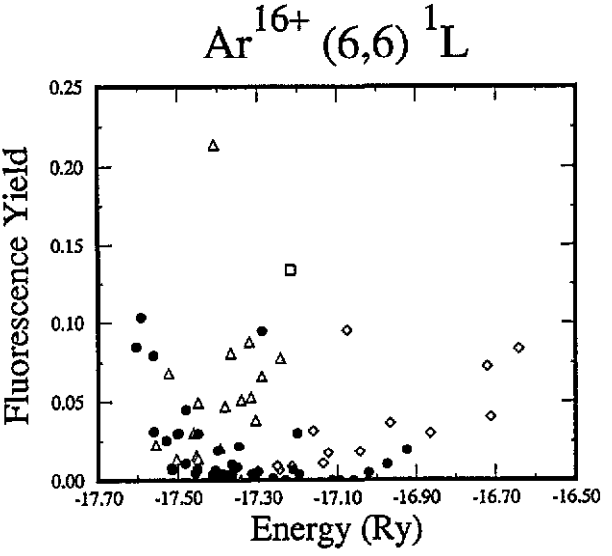

Figure 4. The same as figure 2, but for the $(6,6)$ manifold of Ar^{16+}. The open squares are for states with $K < 0$ and $\eta = -$.

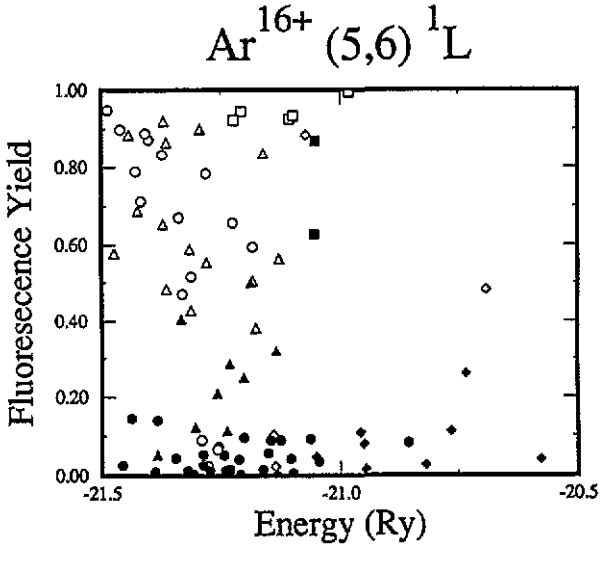

Figure 5. The fluorescence yields of all the singlet states of the $(5,6)$ manifold of Ar^{16+}. The full symbols are for $A = +$ states and open ones for $A = -1$ and $A = 0$ states. The circles are for $K > 0$ and $\eta = +$, the triangles are for $K > 0$ and $\eta = -$, the diamonds are for $K < 0$ and $\eta = +$ and the squares are for $K < 0$ and $\eta = -$.

by Cederquist *et al* (1992) and others. The simple extended over-the-barrier model (Niehaus 1986) predicts that the double electron capture process tends to populate two excited electrons with nearly identical principal quantum numbers, $n \cong N$. If the (N, n) manifold does not overlap with other (N', n') manifolds where $n' \gg N'$, then the fluorescence yield is expected to be small. However, overlapping resonances

are quite common for large n and N and thus large fluorescence yields are expected (Roncin *et al* 1991). Secondly, the $n \neq N$ manifolds can also be populated directly by the double capture process. For example, in the O^{8+}–He collisions at low energies, the cross section of capture to the (3,4) manifold is larger than that to the (3,3) manifold (Bliman *et al* 1983, Barat *et al* 1987, Moretto-Capelle *et al* 1989, Chen *et al* 1991). As the charge state q of the incident ion increases, both the number of manifolds as well as the principal quantum numbers of the (N, n) manifolds with $n \neq N$ increase. These intershell manifolds have large number of $A = -1$, and 0 states, and thus the average fluorescence yield increases as q increases.

4. Conclusions

In summary, we calculate the fluorescence yields of high-lying intrashell and intershell doubly excited states. These data are very useful in understanding the large fluorescence yields obtained in double electron capture of highly charged ions colliding with atoms or scattering on surfaces. If the mixing due to different manifolds is neglected, it is shown that the fluorescence yields of intrashall doubly excited states are small and decrease rapidly with increasing principal quantum number N. However, for high-lying doubly excited states, the intrashell states are often degenerate with intershell states and the latter have states with large fluorescence yields if $A = -1$ or 0. The existence of a large average fluorescence yield is an indication that these $A = -1$ and $A = 0$ intershell states are formed in double capture processes. This is in contrast to doubly excited states formed by photoabsorption or by electron impact where it is well known that only the $A = +1$ states are predominantly formed (Domke *et al* 1991).

Acknowledgments

This research was supported in part by the US Department of Energy, Office of Energy Sciences, Office of Basic Energy Research, Division of Chemical Sciences.

References

Ali R 1992 Private communication

Barat M, Gaboriaud M N, Guillemot L, Roncin P, Laurent H and Andriamonje S 1987 *J. Phys. B: At. Mol. Phys.* **20** 5771

Barat M and Roncin P 1992 *J. Phys. B: At. Mol. Opt. Phys.* **25** 2205

Bliman S, Hitz D, Jacquot B, Harel C and Salin A 1983 *J. Phys. B: At. Mol. Phys.* **16** 2849

Cederquist H *et al* 1992 *Phys. Rev.* A **46** 2592

Chen Z, Shingal R and Lin C D 1991 *J. Phys. B: At. Mol. Opt. Phys.* **24** 4215

Domke M, Xue C, Puschmann A, Mandel T, Hudson E, Shirley D A Kaindl G, Greene C H, Sadeghpour H R and Peterson H 1991 *Phys. Rev. Lett.* **66** 1306

Gou B, Chen Z and Lin C D 1991 *Phys. Rev.* A **43** 3262

Lin C D 1986 *Adv. At. Mol. Phys.* **22** 77

Luc-Koenig E and Bauche J 1990 *J. Phys. B: At. Mol. Opt. Phys.* **23** 1763

Moretto-Capelle P, Oza D H, Benoit-Cattin P, Bordenave-Montesquieu A, Boudjema M, Gleizes A, Dousson S and Hitz D 1989 *J. Phys. B: At. Mol. Opt. Phys.* **22** 271

Niehaus A 1986 *J. Phys. B: At. Mol. Phys.* **19** 2925

Roncin P, Gaboriaud M N and Barat M 1991 *Europhys. Lett.* **16** 551

Tang J, Watanabe S, Matsuzawa M and Lin C D 1992 *Phys. Rev. Lett.* **69** 1633